frontiers | Frontiers in Control Engineering

TYPE Original Research
PUBLISHED 24 November 2022
DOI 10.3389/fcteg.2022.1008134

OPEN ACCESS

EDITED BY
Dipankar Deb,
Institute of Infrastructure, Technology, Research and Management, India

REVIEWED BY
Fadi Dohnal,
Vorarlberg University of Applied Sciences, Austria
Zheng Li,
Hebei University of Science and Technology, China

*CORRESPONDENCE
Syed Muhammad Amrr,
syedamrr@gmail.com

SPECIALTY SECTION
This article was submitted to Adaptive, Robust and Fault Tolerant Control, a section of the journal Frontiers in Control Engineering

RECEIVED 31 July 2022
ACCEPTED 04 November 2022
PUBLISHED 24 November 2022

CITATION
Saha S, Amrr SM, Bhutto JK, AlJohani AA and Nabi M (2022), Fuzzy logic control of five-DOF active magnetic bearing system based on sliding mode concept. *Front. Control. Eng.* 3:1008134. doi: 10.3389/fcteg.2022.1008134

Fuzzy logic control of five-DOF active magnetic bearing system based on sliding mode concept

Sudipta Saha[1], Syed Muhammad Amrr[1,2]*, Javed Khan Bhutto[3], Anas Ayesh AlJohani[3] and M. Nabi[1]

[1]Department of Electrical Engineering, Indian Institute of Technology Delhi, New Delhi, India, [2]Department of Electrical Engineering, Qatar University, Doha, Qatar, [3]Department of Electrical Engineering, College of Engineering, King Khalid University, Abha, Saudi Arabia

In rotor dynamics, the deviation of the shaft is a common phenomenon. The main reasons for the deviation are non-linear attractive forces, harmonic disturbances, system parameter variations, etc. Active magnetic bearings (AMBs) are used to support the rotor inside the air gap in rotating machines, thus avoiding wear and tear and possible breakdowns. This paper proposes a fuzzy sliding mode-inspired control (FSMIC) technique for the five-degrees-of-freedom (DOF) AMB system in the presence of system uncertainties and measurement noises. The fuzzy logic is used to estimate the auxiliary control input of the sliding mode control (SMC) to attenuate the chattering. The variable gains are designed with the help of superintended fuzzy logic to bring more flexibility to the controller performance. The stability analysis is presented with the help of the Lyapunov function candidate. The simulation studies for the AMB system under distinct types of control techniques, i.e., PID, SMC, and FSMIC, illustrate the effectiveness of the proposed control strategy.

KEYWORDS

fuzzy logic, sliding mode control, active magnetic bearing, gain estimation, MIMO, stabilization

1 Introduction

A magnetic bearing is a specific type of bearing which holds the rotor without physical contact with the stator, using electromagnets. Magnetic bearings that are controlled by a feedback control system are referred to as active magnetic bearings (AMBs). Conventional mechanical bearings were used in the industries to support the shaft with the help of physical contact or fluid films. In many critical applications (Bleuler et al., 2009), particularly those involving high-speed rotation, AMB systems have proved a better alternative in recent years. The advantages of AMB are efficient energy consumption, low friction losses, noise-free operation, longer lifetime, etc. (Saha and Nabi, 2016; Peng and Zhou, 2019; Saha et al., 2019).

Some examples of the use of the AMB system in different industrial applications are mentioned in the following text. In a study by Scharfe et al. (2001), a magnetically suspended momentum wheel was designed for aerospace applications, specifically to

support small and medium satellites. A flywheel-based energy storage system built on superconducting AMB was presented by Koshizuka et al. (2003). In a study by Knospe (2007), a high-speed machine spindle for the application of metal cutting was discussed. An axial AMB-based blood pump was designed by Ricci et al. (2016) for medical industry application. AMB is also used extensively for turbomachines (Aenis et al., 2002) and to support rotor dynamics (Tang et al., 2014).

Most AMB systems encounter problems such as vibration phenomena, mass imbalance, and harmonic disturbances (Esfahani et al., 2013; Liu et al., 2019). Moreover, in general, the AMB system is unstable and uncertain. Hence, the use of control techniques for the balance and control of the AMB system is crucial. A significant amount of research has been reported in the recent decades by Mushi et al. (2011) and Noshadi et al. (2014) to stabilize and regulate the AMB system.

The literature has few reports of control technique applications to the AMB system. The decentralized nature of classical control strategies such as PI/PD allows for controlling the shaft's location of the AMB system (Polajžer et al., 2006). The gains of classical control techniques such as the proportional integral derivative controller (PID) are normally fixed. Thus, nowadays, PID control is combined with other control techniques to update the gains. In studies by Chen et al. (2009) and Chang and Chen (2009), a way to update the fixed gains by using fuzzy logic and an adaptive genetic algorithm has been presented. However, the performance of PID control is affected when the system dynamics contain uncertainties. Therefore, in a study by Kang et al. (2011), an LMI-based H_∞ control was proposed for the regulation of the AMB system. Also, H_∞ control of the AMB system was presented by Cole et al. (2017) after considering the vibration of rotor dynamics. The model predictive control for the AMB was discussed by Huang et al. (2007) and Bonfitto et al. (2018). De Miras et al. (2013) investigated the use of model-free control in the aspects of the AMB system. The adaptive control strategy has also been used to control the AMB system with a moving base (Sivrioglu, 2007).

The deviations of the rotor from the nominal position and unbalancing due to mass imbalance are the main challenges in the case of control of the AMB system. To tackle these phenomena, sliding mode control (SMC) has been used in different research works because of the advantages of robustness, faster convergence, ease of design, and better transient and steady-state responses (Edwards and Spurgeon, 1998; Amrr et al., 2022a). In a study by Kang et al. (2010), a conventional SMC is implemented for the AMB system with a movable base that only ensures the asymptotic convergence of system states. An integral SMC control for the regulation problem of the five-degrees-of-freedom (DOF) AMB system is presented in a study by Lin et al. (2011), where the gains are updated using a neural network. In the aforementioned SMC techniques, the issue of the chattering phenomenon (Shtessel et al., 2014) is mainly addressed using the boundary layer technique. This technique resolves the problem of chattering at the cost of the robustness of SMC (Amrr et al., 2022c). Another effective approach to address the chattering is a higher-order SMC scheme (Levant, 2003; Davila et al., 2005; Defoort et al., 2009; Utkin et al., 2020). The higher-order SMC strategies have also been used for the uncertain AMB system, and the recent results were reported by Saha et al. (2020), Amrr and Alturki (2021), and Saha et al. (2021). In a study by Saha et al. (2020), an adaptive-based second-order SMC was designed, whereas Saha et al. (2021) extended this result to a third-order SMC approach. Likewise, non-singular fast terminal sliding surface-based second-order SMC was proposed by Amrr and Alturki (2021) and Amrr et al. (2022b) to resolve the issue of chattering. Although these schemes are effective in solving the problem of unwanted chattering, they have high computational complexities, the control design is mathematically intensive, and it also requires an additional differential observer to estimate the higher-order derivatives of system states (Saha et al., 2020; Saha et al., 2021).

The chattering in SMC arises due to the switching characteristics, so a good alternative to this is the use of the approximation method. Therefore, a worthwhile approximation method to attenuate the chattering is the auxiliary control by the fuzzy logic algorithm (Lo and Kuo, 1998; Tong and Li, 2003). Since Lotfi A. Zadeh originally proposed fuzzy logic (FL) and fuzzy set theory in the 1970s, they have drawn much interest from scholars as an emerging field. FL has been employed in a variety of applications, including control, communication, the creation of integrated circuits, and medical fields. However, fuzzy logic control (FLC) has been the most effective application of FL. Numerous scholars have looked at the possibility of fuzzy control applications for active magnetic bearing control (Alassar et al., 2010; Amer et al., 2011; Su and Li, 2016). Fuzzy logic control has also been explored for the modeling of the AMB system from its input–output relation and combined with SMC for robust control of the system under gyroscopic effects, as can be seen in the study by Xu and Nonami (2003). The primary characteristic of FLC is the use of IF-THEN rules that are based on conventional control theories and human experiences. Such FL principles can be used to tackle chattering issues in traditional SMC theory. The fuzzy-based SMC (FSMC) combines FL and SMC theories and provides the benefits of both SMC and FLC (Palm, 1994; Li et al., 1997). The FSMC scheme is highly efficient in lowering the number of switches in the SMC approach without compromising the other system performances. By using the linguistic fuzzy rules, the system state trajectory may be brought back to the defined sliding surface by choosing either a big or tiny control force as it moves away from the sliding surface.

Fuzzy sliding mode control of a single DOF AMB system was presented in a study by Qin et al. (2011), where the tracking problem was effectively tackled. The reference tracking of the

rotor was first performed using only nominal control input, and then to solve the problem of chattering, fuzzy logic was used along with the sliding mode control. However, the use of fuzzy sliding mode control for the stabilization of the MIMO AMB system has not been explored previously. Thus, this paper proposes a fuzzy SMC-inspired control with variable gain for the stabilization of the five-DOF AMB system, which, to the authors' knowledge, has not been previously explored much.

The contributions of this paper can be summarized as follows:

- A fuzzy-based sliding mode-inspired control is designed for the regulation problem of the five-DOF AMB system subjected to the system uncertainties and measurement noise.
- The auxiliary control input is calculated using a Mamdani-based fuzzy inference with two inputs and one output to attenuate the chattering phenomenon, the auxiliary control input is estimated by two inputs one output Mamdani-based fuzzy inference engine. Also, a superintended fuzzy block is used to update the auxiliary control gains to bring flexibility to the controller design.
- Three different types of control techniques (PID, SMC, and FSMIC) have been compared for the AMB system to provide efficacy and validate the proposed control technique.

The paper is categorized as follows: the system descriptions for five-DOF AMB systems are introduced in the first section, and in the second section, the problem formulation is presented. In the next section, a fuzzy-based SMC-inspired control with a variable gain is proposed, and Lyapunov-based stability analysis is presented. The simulation results are discussed in the next section. Finally, the conclusion is drawn in the last section.

2 Five-DOF AMB system

Figure 1 shows a simplified version of the model given by Lin et al. (2011). The essential components are two identical radial AMBs (RAMBs) and a thrust AMB (TAMB) in addition to the motor and the shaft. The two RAMBs are used in the two endpoints of the shaft to control four DOF, and the TAMB is used to control the axial DOF.

The measurement of the shaft anomaly in the X–Y direction from the nominal air gap is detected by sensors placed in the two RAMBs. The shaft deviation in the Z direction is sensed by a single sensor installed in the TAMB. The sensors send the measurement signals to the controller, and, based on these deviations, the controller generates a control signal to make the deviations zero.

The system dynamics can be represented as follows after decoupling the coupling of the five axes (Sivrioglu, 2007; Lin et al., 2011):

$$\boldsymbol{M}\ddot{\boldsymbol{x}} = \boldsymbol{A}\boldsymbol{x} + \boldsymbol{B}\boldsymbol{u} + \boldsymbol{M}\boldsymbol{q}, \tag{1}$$

where $\boldsymbol{x} = [x_1\ x_2\ y_1\ y_2\ z]^T$ presents states, which actually are the deviations in the shaft in the five axes; $\boldsymbol{u} = [i_{x1}\ i_{x2}\ i_{y1}\ i_{y2}\ i_z]^T$ displays control input currents; and Eq. 5 presents the term due to decoupling $\boldsymbol{q} = [q_{x1}\ q_{x2}\ q_{y1}\ q_{y2}\ q_z]^T$. The mass matrix ($\boldsymbol{M}$), stiffness matrix ($\boldsymbol{A}$), and control gain matrix ($\boldsymbol{B}$) matrices are presented as follows (Lin et al., 2011; Abooee and Arefi, 2019):

$$\boldsymbol{M} = \boldsymbol{I}_{5\times5}, \tag{2}$$

$$\boldsymbol{A} = \mathrm{diag}\left[k_{fp}\vartheta_1,\ k_{fp}\vartheta_3,\ k_{fp}\vartheta_1,\ k_{fp}\vartheta_3,\ k_{tp}\vartheta_4\right], \tag{3}$$

$$\boldsymbol{B} = \mathrm{diag}\left[k_{fi}\vartheta_1,\ k_{fi}\vartheta_3,\ k_{fi}\vartheta_1,\ k_{fi}\vartheta_3,\ k_{ti}\vartheta_4\right], \tag{4}$$

$$\boldsymbol{q} = \begin{bmatrix} -\varepsilon_1\dot{y}_1 + \varepsilon_1\dot{y}_2 + 2k_{fp}\vartheta_2x_2 + 2k_{fi}\vartheta_2i_{x2} + \varrho_1 f_{dtx} \\ \varepsilon_2\dot{y}_1 - \varepsilon_2\dot{y}_2 + 2k_{fp}\vartheta_2x_1 + 2k_{fi}\vartheta_2i_{x1} + \varrho_2 f_{dtx} \\ \varepsilon_1\dot{x}_1 - \varepsilon_1\dot{x}_2 + 2k_{fp}\vartheta_2y_2 + 2k_{fi}\vartheta_2i_{y2} + \varrho_1 f_{dty} - g \\ -\varepsilon_2\dot{x}_1 - \varepsilon_2\dot{x}_2 + 2k_{fp}\vartheta_2y_1 + 2k_{fi}\vartheta_2i_{y1} + \varrho_2 f_{dty} - g \\ \varrho_3 f_{dtz} \end{bmatrix}, \tag{5}$$

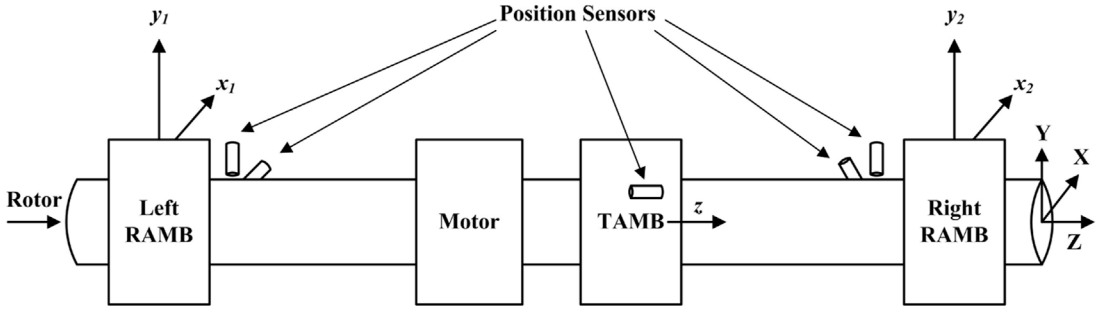

FIGURE 1
Sketch of a five-DOF AMB system.

where k_{fp}, k_{fi}, k_{tp}, and k_{ti} are the stiffness related to position and current of the RAMB and the TAMB, respectively, while $\vartheta_1 = (\frac{1}{m}) + (\frac{a^2}{J})$, $\vartheta_2 = (\frac{1}{m}) - (\frac{ab}{J})$, $\vartheta_3 = (\frac{1}{m}) + (\frac{b^2}{J})$, and $\vartheta_4 = (\frac{1}{m})$, where mass of rotor is denoted by m, and the parameters a, b, and c are the distances to the center of gravity (CG) from the left RAMB, the right RAMB, and the end of rotor, respectively. The transverse moment of inertia is denoted as J, the polar moment of inertia is given as J_z, and $\varepsilon_1 = \frac{aJ_z\omega}{Jl}$, $\varepsilon_2 = \frac{bJ_z\omega}{Jl}$ with l being the distance between two RAMBs and $\varrho_1 = (\frac{1}{m}) - (\frac{ac}{J})$, $\varrho_2 = (\frac{1}{m}) + (\frac{bc}{J})$, and $\varrho_3 = (\frac{1}{m})$. Finally, external disturbance forces are considered as f_{dtx}, f_{dty}, and f_{dtz}.

To derive a control law for the fuzzy SMC, first, the system dynamics have to be formulated as first-order dynamics. The problem formulation for converting the first-order dynamics is discussed in the following section.

3 Problem formulation

Initially, the non-linear five-degrees-of-freedom AMB is converted into a linear model, and the coupling of states is removed by decoupling the dynamics. The parameters in system dynamics often fluctuate. Therefore, system dynamics will always suffer from some amount of uncertainty. In the case of practical applications, approximating the precise nominal values of system matrices $\boldsymbol{A}$ and $\boldsymbol{B}$ is challenging. Moreover, the decoupled term q can be considered as an uncertainty. Therefore, the nominal system parameters along with the uncertainties are presented as

$$\begin{aligned}\ddot{\boldsymbol{x}} &= [\boldsymbol{A}_{nom} + \Delta\boldsymbol{A}]\boldsymbol{x}(t) + [\boldsymbol{B}_{nom} + \Delta\boldsymbol{B}]\boldsymbol{u}(t) + \boldsymbol{q}(t)\\ &= \boldsymbol{A}_{nom}\boldsymbol{x}(t) + \boldsymbol{B}_{nom}\boldsymbol{u}(t) + \boldsymbol{n}(t),\end{aligned} \tag{6}$$

where $\boldsymbol{A}_{nom}$ and $\boldsymbol{B}_{nom}$ are the nominal values of $\boldsymbol{A}$ and $\boldsymbol{B}$, respectively, the variations of time-varying system parameters are symbolized as $\Delta\boldsymbol{A} \in \mathbb{R}^{5\times5}$ and $\Delta\boldsymbol{B} \in \mathbb{R}^{5\times5}$, and the lumped uncertainty denoted as $\boldsymbol{n} \in \mathbb{R}^{5\times1}$ is presented as

$$\boldsymbol{n}(t) = \Delta\boldsymbol{A}\boldsymbol{x}(t) + \Delta\boldsymbol{B}\boldsymbol{u}(t) + \boldsymbol{q}(t). \tag{7}$$

Assumption 1: The system states and its derivatives are measurable during the designing feedback.

Assumption 2: The variable $\boldsymbol{n}$ is slowly time-varying and bounded, i.e., $\|\boldsymbol{n}\| \le \underline{n}$ and the values of $\underline{n} > 0$ are known.

Remark 1: The first-order derivative of states $\boldsymbol{x}$ can be derived by using a finite-time differentiator (Levant, 2007). This observer estimates the derivative of the input signal, and it is expressed as

$$\dot{\boldsymbol{\varphi}}_1 = -c_1|\boldsymbol{\varphi}_1 - \boldsymbol{x}|^{\frac{1}{2}}\boldsymbol{sign}(\boldsymbol{\varphi}_1 - \boldsymbol{x}) + \boldsymbol{\varphi}_2, \tag{8a}$$

$$\dot{\boldsymbol{\varphi}}_2 = -c_2\boldsymbol{sign}(\boldsymbol{\varphi}_2 - \boldsymbol{x}), \tag{8b}$$

where $c_1 > 0$, $c_2 > 0$, and $c_1 > c_2$. The variables $\boldsymbol{\varphi}_1 \in \mathbb{R}^5$ and $\boldsymbol{\varphi}_2 \in \mathbb{R}^5$ are the estimates of $\boldsymbol{x}$ and $\dot{\boldsymbol{x}}$, respectively.

Now, the system dynamics Eq. 6 is converted into first-order dynamics by using Eq. 9 as follows:

$$\boldsymbol{x}_1 \in \mathbb{R}^5 = \boldsymbol{x} \text{ and } \boldsymbol{x}_2 \in \mathbb{R}^5 = \dot{\boldsymbol{x}}. \tag{9}$$

Substituting these new variables in Eq. 6 yields

$$\begin{aligned}\dot{\boldsymbol{x}}_1 &= \boldsymbol{x}_2\\ \dot{\boldsymbol{x}}_2 &= \boldsymbol{A}_{nom}\boldsymbol{x}_1 + \boldsymbol{B}_{nom}\boldsymbol{u}(t) + \boldsymbol{n}.\end{aligned} \tag{10}$$

Therefore, the main objective of the controller design is to stabilize the shaft in the nominal air gap by navigating the state variables (x_1, x_2, y_1, y_2, z) and its derivatives to zero despite system uncertainties and measurement noise, i.e.,

$$\lim_{t\to\infty}(\boldsymbol{e}) = [0\ 0\ 0\ 0\ 0]^T, \tag{11}$$

$$\lim_{t\to\infty}(\dot{\boldsymbol{e}}) = [0\ 0\ 0\ 0\ 0]^T, \tag{12}$$

where the error is $\boldsymbol{e} \in \mathbb{R}^{5\times1} = \boldsymbol{x}_1 - \boldsymbol{x}_d$, and $\boldsymbol{x}_d$ is the central position in AMB. To achieve this objective, a fuzzy logic controller inspired by sliding mode is proposed in the next section.

4 The proposed control strategy

In this section, first, the fuzzy logic-based control law is designed, and the subsequent Lyapunov-based stability analysis is presented.

Sliding mode control is a non-linear technique that helps the system dynamics perform in a prescribed manner despite uncertainties. In this technique, the system dynamics are forced to reach a sliding surface and then slide on it. The most crucial part of designing the SMC is to choose the sliding surface carefully. Due to the flexibility of choosing proportional integral derivative (PID) gains in SMC control (Stepanenko et al., 1998), in this paper, a PID sliding surface is selected over a linear sliding surface to design an SMC-inspired controller. A PID sliding surface based on the error in the states can be presented as (Eker, 2006)

$$\boldsymbol{s}(t) = \boldsymbol{K}_p\boldsymbol{e}(t) + \boldsymbol{K}_i\int\boldsymbol{e}(\zeta)d\zeta + \boldsymbol{K}_d\frac{d}{dt}\boldsymbol{e}(t), \tag{13}$$

where $\boldsymbol{K}_p \in \mathbb{R}^{5\times5}$ is matrix of proportional gain, $\boldsymbol{K}_i \in \mathbb{R}^{5\times5}$ is matrix of integral gain, and $\boldsymbol{K}_d \in \mathbb{R}^{5\times5}$ is matrix of derivative gain. For the five-DOF AMB system, $\boldsymbol{K}_p$, $\boldsymbol{K}_i$, and $\boldsymbol{K}_d$ can be defined as

$$\begin{aligned}\boldsymbol{K}_p &= \mathrm{diag}\left[k_{p1}\ k_{p2}\ k_{p3}\ k_{p4}\ k_{p5}\right]\\ \boldsymbol{K}_i &= \mathrm{diag}[k_{i1}\ k_{i2}\ k_{i3}\ k_{i4}\ k_{i5}]\\ \boldsymbol{K}_d &= \mathrm{diag}[k_{d1}\ k_{d2}\ k_{d3}\ k_{d4}\ k_{d5}].\end{aligned} \tag{14}$$

After getting $\boldsymbol{s}$ from Eq. 13, the change in sliding surface variable $\dot{\boldsymbol{s}}$ can be generated through signal processing.

In the absence of uncertainties ($\boldsymbol{n}$) and taking $\dot{\boldsymbol{s}} = 0$, the nominal control input can be designed. Now, the nominal control input $\boldsymbol{u}_n$ can be presented as

$$\boldsymbol{u}_n = (\boldsymbol{K}_d\boldsymbol{B}_{nom})^{-1}\left(-\boldsymbol{K}_p\dot{\boldsymbol{e}} - \boldsymbol{K}_i\boldsymbol{e} - \boldsymbol{K}_d\boldsymbol{A}_{nom}\boldsymbol{x}_1\right), \tag{15}$$

where $\boldsymbol{K}_d\boldsymbol{B}_{nom}$ is invertible as both $\boldsymbol{K}_d$ and $\boldsymbol{B}_{nom}$ are diagonal. In the presence of uncertainties, an additional control input called auxiliary control is needed to suppress the uncertainties. Also, the auxiliary control is the main reason for the chattering problem in SMC control. To contain the chattering problem, the auxiliary control in this paper is estimated by fuzzy logic.

Fuzzy logic control (FLC) has been applied to many practical applications. The significant advantage of employing fuzzy logic is that it can transform the amount of vagueness into a human-understandable form (Bai and Roth, 2019). Therefore, in the absence of a mathematical model or mathematical model containing uncertainties, the issue can be efficiently dealt with by using fuzzy logic control. However, large numbers of rule base for higher-order systems complicate the analysis. Thus, much focus has been given to fuzzy SMC control (Yau and Chen, 2006; Roopaei and Jahromi, 2009; Lin et al., 2019).

To suppress the chattering phenomenon, a fuzzy inference engine along with a fuzzy rule base is used, and FSMIC is proposed, which is similar to the design in studies by Yau and Chen (2006) and Roopaei and Jahromi (2009). Along with the estimation of auxiliary control input, the gain used for auxiliary control is also estimated using a fuzzy inference engine for the improvement of the system performance. This type of gain modification is normally known as superintended fuzzy control. The robustness of the system behavior is the main advantage of this method. The block diagram of fuzzy SMC-inspired control is shown in Figure 2. Fuzzy SMC block and superintended fuzzy block each consist of five components, where only one component of each block is shown in Figures 3 and 4, respectively. The Mamdani-

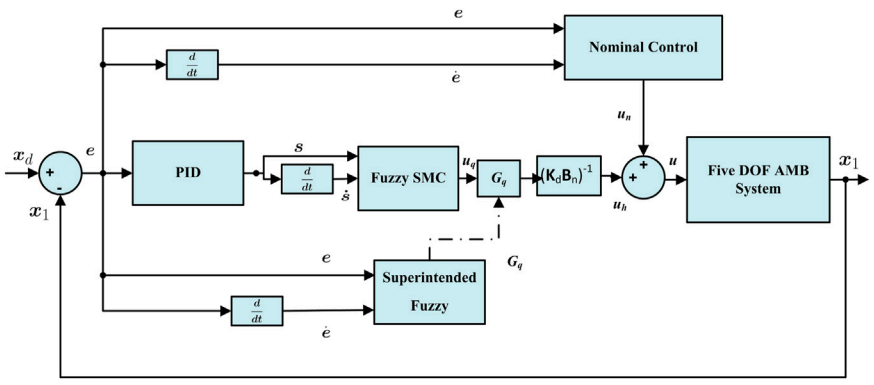

FIGURE 2
Fuzzy SMC-inspired control with PID surface.

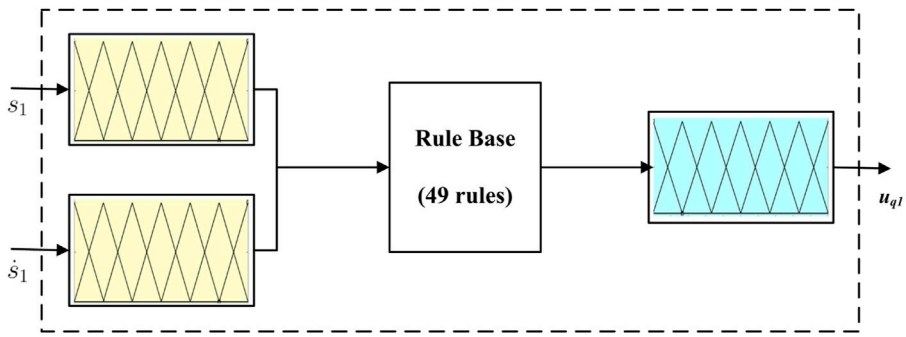

FIGURE 3
Fuzzy SMC block.

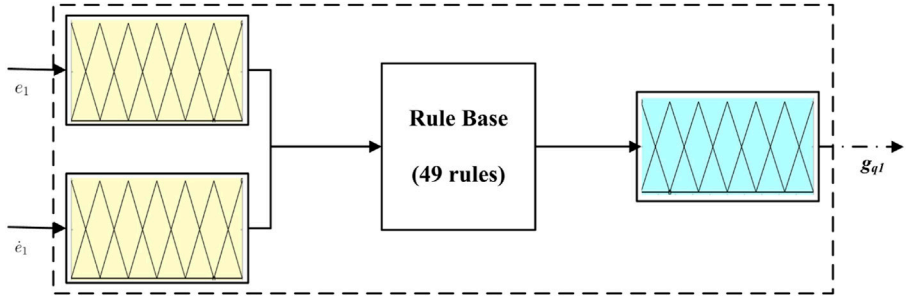

FIGURE 4
Superintended fuzzy block.

based fuzzy inference method is used for both blocks to construct the two-input-one-output setup. In the case of fuzzy SMC block, inputs are sliding surface variable (s_1) and change in sliding surface ($\dot{s}_1$) and the output is the main component of calculated auxiliary control u_{q1}. In the superintended block, inputs are the error and change in error, and the output is the variable gain for auxiliary control.

The auxiliary control law is designed as

$$\boldsymbol{u}_h = (\boldsymbol{K}_d \boldsymbol{B}_{nom})^{-1}\left(\boldsymbol{G}_q \boldsymbol{u}_q\right), \tag{16}$$

where $\boldsymbol{G}_q$ is the auxiliary control gain which can be represented as $\boldsymbol{G}_q = \text{diag}\{g_{q1}, g_{q2}, g_{q3}, g_{q4}, g_{q5}\}$, and $\boldsymbol{u}_q$ is the output of fuzzy SMC block. The rules for the fuzzy control are produced by mapping input variables $(\boldsymbol{s}, \dot{\boldsymbol{s}})$, which are linguistic in nature, to the output linguistic variable $\boldsymbol{u}_q$ by the following relation (Roopaei and Jahromi, 2009):

$$\begin{aligned}\boldsymbol{u}_q &= \left[u_{q1}(s_1, \dot{s}_1),\ u_{q2}(s_2, \dot{s}_2),\ \cdots,\ u_{q5}(s_5, \dot{s}_5)\right]^T \\ &= \left[u_{qi}(s_i, \dot{s}_i)\right],\end{aligned} \tag{17}$$

where $i = 1, 2, \ldots, 5$.

The fuzzy membership functions and fuzzy rule base are designed for the fuzzy SMC and superintended block. Here, the fuzzy design of only one component inside those blocks is shown. However, the design for other components is the same as that for this one. The input variables (s_1, $\dot{s}_1$) and output variable main component of auxiliary control (u_{q1}) which are linguistic in nature are represented by membership functions, as shown in Figure 5. The inputs and output are mapped into the domain [−1, 1] and divided into seven fuzzy divisions, which are represented as "BN" (big negative), "MN" (medium negative), "SN" (small negative), "ZE" (zero), "SP" (small positive), "MP" (medium positive), and "BP" (big positive). The fuzzy rules are selected such that the controller stability is preserved. The rules are selected by IF-THEN logic by taking s_1 and $\dot{s}_1$ as inputs and u_{q1} as output (Zadeh, 1965; Wang and Mendel, 1992). The rule base for fuzzy SMC is given in Table 1, where $i = 1, \ldots, 5$. The whole

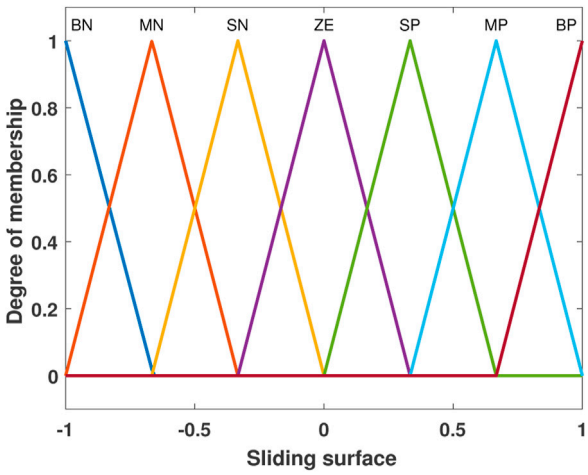

FIGURE 5
Membership function for sliding surface (s_1), change in s_1 ($\dot{s}_1$), and auxiliary control (u_{q1}).

fuzzification is performed using the singleton process, and the crisp value of the output is generated by center average defuzzification.

For the construction of the superintended fuzzy block, two inputs, which are errors (e_1 and $\dot{e}_1$), are fuzzified in the same manner as was performed for the fuzzy SMC. The membership function of the inputs is given in Figure 6. The range of the inputs is taken as [−0.01, 0.01]. The output of the superintended fuzzy block is also fuzzified and divided into seven divisions represented as "VVT" (very very tiny), "VT" (very tiny), "T" (tiny), "M" (medium), "L" (large), "VL" (very large), and "VVL" (very very large). The membership function of the output is given in Figure 7. The range of the output is taken as [1000, 6000]. The surface view for the superintended fuzzy control for gain estimation is shown in Figure 8. The fuzzy rules for this block are also based on IF-THEN conditions, and rules are generated by the Mamdani

TABLE 1 Rule base for fuzzy SMC block.

	s_i					
$\dot{s}_i$	**BP**	**MP**	**SP**	**ZE**	**SN**	**MN**
BP	BN	BN	BN	ZE	ZE	ZE
MP	BN	BN	BN	ZE	ZE	ZE
SP	BN	BN	MN	ZE	ZE	SP
ZE	BN	MN	SN	ZE	SP	MP
SN	MN	SN	ZE	ZE	MP	BP
MN	SN	ZE	ZE	ZE	BP	BP
BN	ZE	ZE	ZE	ZE	BP	BP

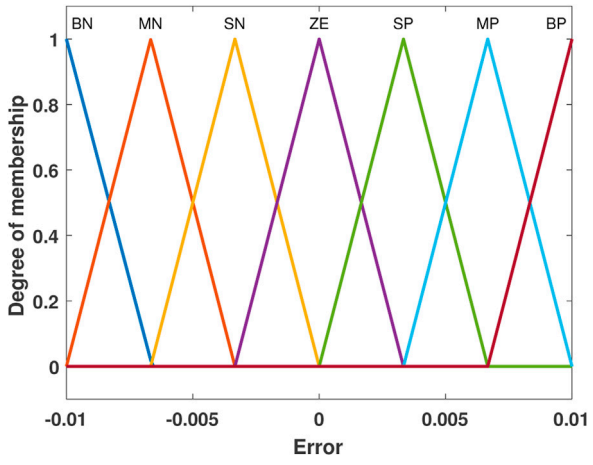

FIGURE 6
Membership function for error (e_1) and change in error ($\dot{e}_1$).

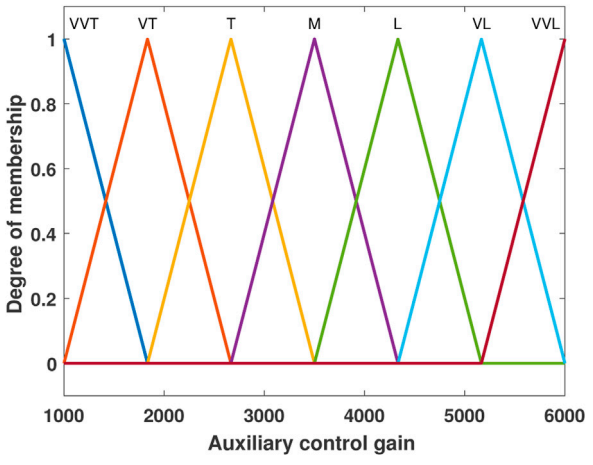

FIGURE 7
Membership function for auxiliary control gain.

method. The rule base for variable gain estimation is given in Table 2. In this case also, the center average defuzzification method is chosen for generating crisp output.

The final control input can be represented as

$$\begin{aligned} \boldsymbol{u} &= \boldsymbol{u}_n + \boldsymbol{u}_h \\ &= (\boldsymbol{K}_d \boldsymbol{B}_{nom})^{-1}\left(-\boldsymbol{K}_p \dot{\boldsymbol{e}} - \boldsymbol{K}_i \boldsymbol{e} - \boldsymbol{K}_d \boldsymbol{A}_{nom} \boldsymbol{x}_1 + \boldsymbol{G}_q \boldsymbol{u}_q\right). \end{aligned} \tag{18}$$

4.1 Stability analysis

Theorem 1: Under Assumptions 1 and 2, the system dynamics (10) can be stabilized to the nominal position using the designed fuzzy-based SMC scheme (18). The proposed control law will steer the states and their derivatives to zero under the influence of model uncertainties and disturbances.

Proof: The stability analysis is presented in two steps. In the first step, the convergence of the sliding surface is proved. Then, the convergence of error and its derivatives is shown.

To show the convergence of the sliding surface, a positive definite Lyapunov function is chosen

$$V_1 = \frac{1}{2}\boldsymbol{s}^T \boldsymbol{s}. \tag{19}$$

Taking the time derivative of Eq. 19,

$$\dot{V}_1 = \boldsymbol{s}^T \dot{\boldsymbol{s}}. \tag{20}$$

After taking the derivative of Eq. 13 and substituting it,

$$\begin{aligned} \dot{V}_1 &= \boldsymbol{s}^T\left(\boldsymbol{K}_p \dot{\boldsymbol{e}} + \boldsymbol{K}_i \boldsymbol{e} + \boldsymbol{K}_d \ddot{\boldsymbol{e}}\right) \\ &= \boldsymbol{s}^T\left(\boldsymbol{K}_p \dot{\boldsymbol{e}} + \boldsymbol{K}_i \boldsymbol{e} + \boldsymbol{K}_d \boldsymbol{A}_{nom} \boldsymbol{x}_1 + \boldsymbol{K}_d \boldsymbol{B}_{nom} \boldsymbol{u} \right. \\ &\quad \left. + \boldsymbol{K}_d \boldsymbol{n}\right). \end{aligned} \tag{21}$$

Now, putting the value of $\boldsymbol{u}$ from Eq. 18, it becomes

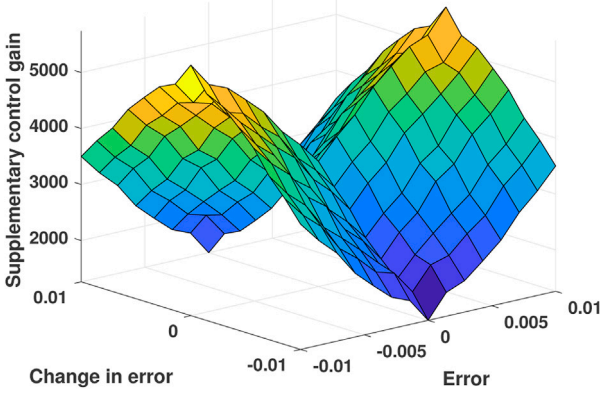

FIGURE 8
Surface view of auxiliary control gain.

$$\begin{aligned}\dot{V}_1 &= \boldsymbol{s}^T\{\boldsymbol{K}_p\dot{\boldsymbol{e}} + \boldsymbol{K}_i\boldsymbol{e} + \boldsymbol{K}_d\boldsymbol{A}_{nom}\boldsymbol{x}_1 + \boldsymbol{K}_d\boldsymbol{B}_{nom} \\ &\quad \cdot(\boldsymbol{K}_d\boldsymbol{B}_{nom})^{-1}\left(-\boldsymbol{K}_p\dot{\boldsymbol{e}} - \boldsymbol{K}_i\boldsymbol{e} - \boldsymbol{K}_d\boldsymbol{A}_{nom}\boldsymbol{x}_1\right. \\ &\quad \left.+\boldsymbol{G}_q\boldsymbol{u}_q\right) + \boldsymbol{K}_d\boldsymbol{n}\} \\ &= \boldsymbol{s}^T\left(\boldsymbol{G}_q\boldsymbol{u}_q + \boldsymbol{K}_d\boldsymbol{n}\right).\end{aligned} \tag{22}$$

The output of the main component of the auxiliary control is mapped in the range of [−1, 1]. So, $|\boldsymbol{u}_q| \le 1$ and $|u_{qi}(s_i,\ \dot{s}_i)| \le 1$. Also, $s_i u_{qi}(s_i,\ \dot{s}_i) \le -|s_i|$ for proposed fuzzy rule base is given in Table 1. Thus, putting the value of the diagonal matrices $\boldsymbol{G}_q$ and $\boldsymbol{K}_d$ and using bound $\|\boldsymbol{n}\| \le \underline{n}$, as given in Assumption 2, Eq. 22 implies

$$\begin{aligned}\dot{V}_1 &= \boldsymbol{s}^T\left(\boldsymbol{G}_q\boldsymbol{u}_q + \boldsymbol{K}_d\boldsymbol{n}\right) \\ &= \left\{g_{q1}s_1\ u_{q1}(s_1,\ \dot{s}_1) + \ g_{q2}s_2\ u_{q2}(s_2,\ \dot{s}_2) + \ \cdots\right. \\ &\quad \left. + \ g_{q5}s_5\ u_{q5}(s_5,\ \dot{s}_5)\right\} + \boldsymbol{s}^T\boldsymbol{K}_d\boldsymbol{n}.\end{aligned} \tag{23}$$

Using the fuzzy SMC rule base in the aforementioned equation, i.e., $s_i u_{qi}(s_i,\ \dot{s}_i) \le -|s_i|$. Therefore,

$$\begin{aligned}\dot{V}_1 &\le -g_{q1}|s_1| - g_{q2}|s_2| - \cdots - g_{q5}|s_5| + \max(k_{d1},\ k_{d2},\ k_{d3},\ k_{d4},\ k_{d5})\ \underline{n}\|\boldsymbol{s}\|_1 \\ &\le -\max\left(g_{q1},\ g_{q2},\ g_{q3},\ g_{q4},\ g_{q5}\right)(|s_1| + |s_2| + |s_3| + |s_4| + |s_5|) \\ &\quad +\max(k_{d1},\ k_{d2},\ k_{d3},\ k_{d4},\ k_{d5})\ \underline{n}\|\boldsymbol{s}\|_1 \\ &= -\max\left(g_{q1},\ g_{q2},\ g_{q3},\ g_{q4},\ g_{q5}\right)\|\boldsymbol{s}\|_1 + \max(k_{d1},\ k_{d2},\ k_{d3},\ k_{d4},\ k_{d5})\ \underline{n}\|\boldsymbol{s}\|_1 \\ &= -\left\{\max\left(g_{q1},\ g_{q2},\ g_{q3},\ g_{q4},\ g_{q5}\right) - \max(k_{d1},\ k_{d2},\ k_{d3},\ k_{d4},\ k_{d5})\ \underline{n}\right\}\|\boldsymbol{s}\|_1 \\ &\le -\eta\|\boldsymbol{s}\|_1, \\ &\le -\eta\left(\|\boldsymbol{s}\|^2\right)^{1/2} \\ &\le -\sqrt{2}\eta\left(\frac{\boldsymbol{s}^T\boldsymbol{s}}{2}\right)^{1/2} \\ &\le -\sqrt{2}\eta V_1^{1/2} < 0,\end{aligned} \tag{24}$$

where $\eta = \{\max(g_{q1},\ g_{q2},\ g_{q3},\ g_{q4},\ g_{q5}) - \max(k_{d1},\ k_{d2},\ k_{d3},\ k_{d4},\ k_{d5})\underline{n}\} > 0$. The closed loop stability is guaranteed subject to the reaching condition, that the gains of $\boldsymbol{G}_q$ should always be greater than $\boldsymbol{K}_d\underline{n}$. Thus, Eq. 24 satisfies the finite-time inequality condition of Bhat and Bernstein (2000). Hence, the sliding surface $\boldsymbol{s}$ converges to zero within finite time.

Once the sliding phase is achieved, i.e., $\boldsymbol{s} = 0$, the AMB system adapts the sliding dynamics. Therefore, Eq. 13 can be represented as

$$\boldsymbol{K}_p\boldsymbol{e}(t) + \boldsymbol{K}_i\int\boldsymbol{e}(\zeta)d\zeta + \boldsymbol{K}_d\frac{d}{dt}\boldsymbol{e}(t) = 0. \tag{25}$$

Now, rearranging the dynamics,

$$\dot{\boldsymbol{e}} = -\boldsymbol{K}_d{}^{-1}\left\{\boldsymbol{K}_p\boldsymbol{e} + \boldsymbol{K}_i\int\boldsymbol{e}(\zeta)d\zeta\right\}. \tag{26}$$

After taking the derivative of Eq. 26,

$$\ddot{\boldsymbol{e}} = -\boldsymbol{K}_d{}^{-1}\boldsymbol{K}_p\ \dot{\boldsymbol{e}} - \boldsymbol{K}_d{}^{-1}\boldsymbol{K}_i\ \boldsymbol{e}. \tag{27}$$

Now, writing Eq. 27 in the state space form,

$$\begin{bmatrix}\dot{\boldsymbol{e}} \\ \ddot{\boldsymbol{e}}\end{bmatrix} = \begin{bmatrix}0 & I \\ -\boldsymbol{K}_d{}^{-1}\boldsymbol{K}_i & -\boldsymbol{K}_d{}^{-1}\boldsymbol{K}_p\end{bmatrix}\begin{bmatrix}\boldsymbol{e} \\ \dot{\boldsymbol{e}}\end{bmatrix}, \tag{28}$$

where the system matrix is in controllable canonical form, and all the coefficients are negative definite, making Eq. 28 a stable system. This proves that the errors and their derivatives will converge to zero asymptotically. In other words, the position of the rotor will asymptotically stabilize to the nominal air gap position.

TABLE 2 Rule base for variable gain.

	e_i						
$\dot{e}_i$	**BN**	**SM**	**SN**	**ZE**	**SP**	**MP**	**BP**
BN	M	T	VT	VVT	VT	T	M
SM	L	M	T	VT	T	M	L
SN	VL	L	M	T	M	L	VL
ZE	VVL	VL	L	M	L	VL	VVL
SP	VL	L	M	T	M	L	VL
MP	L	M	T	VT	T	M	L
BP	M	T	VT	VVT	VT	T	M

5 Numerical analysis

This section presents the performance of the proposed fuzzy sliding mode-inspired control (FSMIC) for an uncertain five-DOF AMB system (10) on the MATLAB simulation platform. In order to establish the effectiveness of the proposed FSMIC design (18), this section also illustrates the comparative simulation analysis with a traditional SMC (Eker, 2006) and proportional integral derivative (PID) control (Ang et al., 2005). The parameter values of AMB system 1) are taken from Lin et al. (2011) and Lin et al. (2010) and given in Table 3. Notably, the rotor is considered to be rigid with a maximum operating speed of 4,800 rpm. The nominal air gap position is taken as $x_b = y_b = 0.4$ mm and $z_b = 0.5$ mm. The bias currents in the coils for RAMB and TAMB are $i_{b_r} = i_{b_l} = 0.9$ A and $i_{b_t} = 1.1$ A, respectively. The initial conditions of five states are $x_1(0) = -0.3$ mm, $x_2(0) = 0.1$ mm, $y_1(0) = 0.25$ mm, $y_2(0) = -0.15$ mm, and $z(0) = 0.2$ mm. The model uncertainties of system parameters (i.e., $\Delta \boldsymbol{A}$ and $\Delta \boldsymbol{B}$) are considered as 10% and 15% of their respective nominal values. To put the effectiveness of the proposed control algorithm to the test, the disturbance forces (f_{dtx}, f_{dty}, f_{dtz}) are taken as

$$\begin{aligned} f_{dtx} &= 0.1\sin(t) + 7 \times 10^{-2}\eta, \\ f_{dty} &= 0.2\sin(5t) + 7 \times 10^{-2}\eta, \\ f_{dtz} &= 0.3\sin(8t) + 7 \times 10^{-2}\eta, \end{aligned} \tag{29}$$

where $\eta \in \mathbb{R}$ is white noise. Furthermore, a random Gaussian white noise with a magnitude of 5×10^{-4} mm is also considered in the state feedback as measurement noise.

5.1 Comparative simulation results

The comparative performances of PID, SMC, and FSMIC are presented through state response, input efforts, and total input variation. The time response of system states, which are rotor positions measured at left and right RAMBs and TAMB, is shown in Figure 9. The state response under PID control, traditional SMC scheme, and FSMIC algorithm are illustrated in the left, middle, and right subplots of Figure 9. It can be seen from the state response under PID and SMC schemes that the rotor deviations settle to zero from the given initial displacement within 0.63 s and 0.51 s, respectively. On the other hand, the proposed FSMIC technique helps converge the states to zero within 0.38 s. Therefore, the convergence rate is faster in the FSMIC scheme than in the comparative

TABLE 3 Five-DOF AMB system parameters (Lin et al., 2011; Lin et al., 2010).

Parameters	Value	Parameters	Value
M	2.56478 kg	a	0.16 m
L	0.505 m	b	0.19 m
D	0.0166 m	c	0.263 m
$\boldsymbol{J}$	0.04004 kg m^2	k_{tp}	36,000 N/m
$\boldsymbol{J}_z$	0.0006565 kg m^2	k_{fi}	80 N/A
L	0.35 m	k_{fp}	220,000 N/m
k_{ti}	40 N/A	ω	48,000 rpm

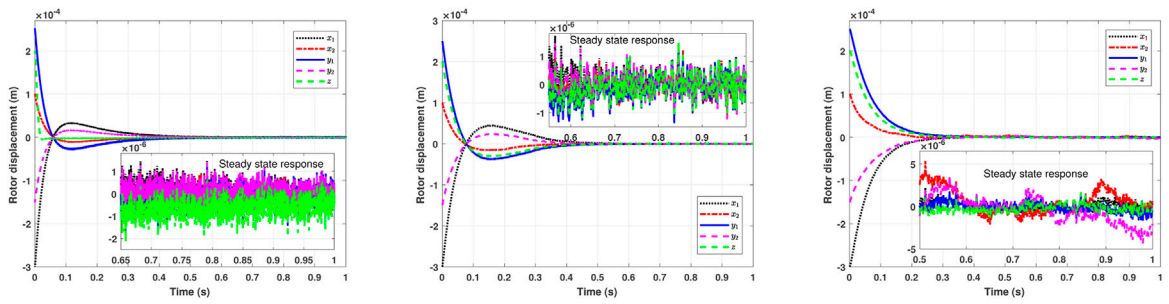

FIGURE 9
States response with PID, SMC, and FSMIC.

approaches. Moreover, there are noticeable overshoot and undershoot in the state trajectories under PID and SMC schemes, whereas there is no overshoot or undershoot in the proposed control strategy. The steady-state response is also presented in the zoomed-in plot in Figure 9, which shows that all the states remain in the neighborhood of zero with the residual bound range of 4×10^{-6} m. The bound of state $\boldsymbol{x}_1$ at the settling time is also mentioned in Table 4, which indicates that the FSMIC algorithm is performing better.

The control inputs' response of these three schemes is shown in Figure 10. In the case of the PID control, the initial control current required is a little higher than the other two schemes, i.e., 1.2 A. Moreover, the transient response in the zoomed-in plot under the PID scheme shows the effect of measurement noise. On the other hand, the traditional SMC scheme experiences a chattering effect which is evident in the transient response. In contrast, the proposed FSMIC approach reduces the chattering to a great extent. The FSMIC scheme circumvents chattering due to the fuzzy-based approximation of the switching function in the sliding mode control design.

In addition, the reduction in input chattering can be quantified by calculating the total variation (TV) input throughout the simulation time. The expression of TV is defined as

$$TV = \sum_{i=1}^{5} \sum_{k=1}^{n} |u_i(k+1) - u_i(k)|, \tag{30}$$

where n is the total number of control input data samples. Figure 11 illustrates the performance of absolute fluctuations of control input over time. In Table 4, the calculated TV values for three control strategies are provided. Therefore, Table 4 and Figure 11 make it clear that the proposed approach has a lesser change in control input than the other two techniques. Consequently, the chattering is significantly minimized in FSMIC design.

The time-varying control gains for the FSMIC scheme are also given in Figure 12. These gains vary between 1,000 and 6,000 and settle down to a constant value when the system reaches a steady state. The value of the gains $\boldsymbol{G}_q$ in the steady state is 5,500. It is important to note that the gains in the PID and SMC controllers are fixed. However, in the FSMIC design, auxiliary control gains are modified using the fuzzy logic algorithm. As a result, the variable gains under the FSMIC approach offer more flexibility over the other two comparative techniques.

Lastly, the amount of control effort executed in achieving the aforementioned results is also evaluated to determine the energy-efficient control performance. Therefore, the energy index value of these three control schemes is calculated using the following formula (Amrr et al., 2020):

$$\text{Energy Index} = \sum_{k}^{5} \int_{s=0}^{s=1} |u_k(s)|^2 ds. \tag{31}$$

The energy index values of the three control schemes are tabulated in Table 4, which shows that the proposed controller consumes the least energy. Hence, the proposed FSMIC algorithm is the most efficient.

TABLE 4 Comparison between different control approaches.

Control techniques	Settling time (s)	$\|\boldsymbol{x}_1\|$ at settling time	Energy index (A^2)	Total variation
PID	0.63	4.0970×10^{-5}	0.0524	439.253
SMC	0.51	2.1033×10^{-5}	0.0320	277.746
FSMIC	0.38	1.0586×10^{-5}	0.0224	165.632

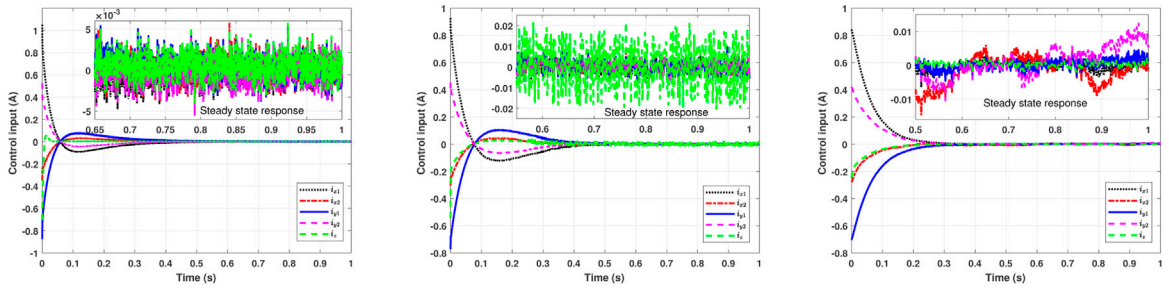

FIGURE 10
Control inputs' response with PID, SMC, and FSMIC.

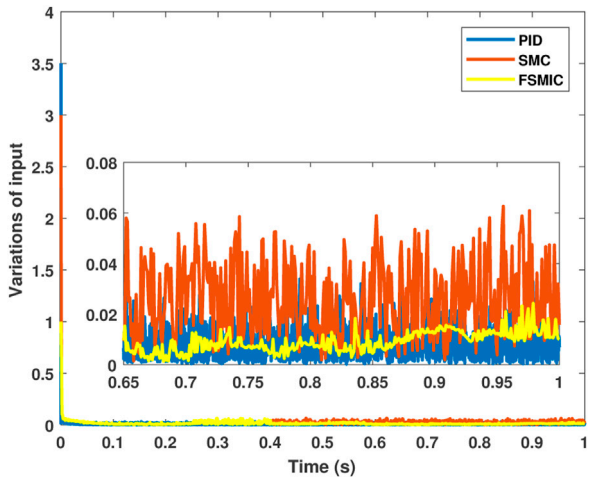

FIGURE 11
Total variations over time for three control techniques.

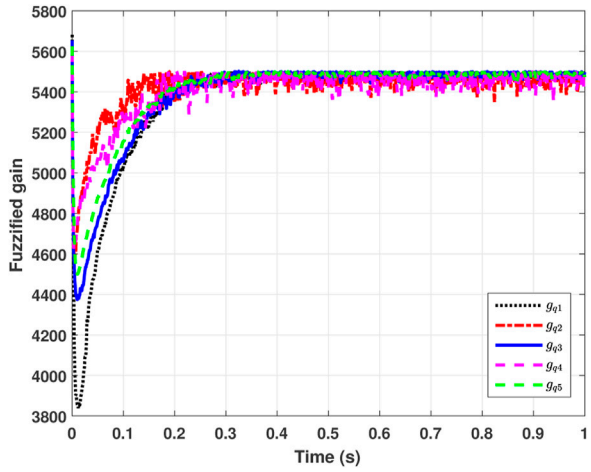

FIGURE 12
Time-varying gain G_q.

6 Conclusion

This paper investigates the application of fuzzy-based SMC for the stabilization of the five-DOF AMB system under parametric uncertainties and disturbances. The fuzzy logic algorithm helps in reducing the chattering effect in the SMC design by approximating the variable gains of the auxiliary control. On the other hand, the SMC provides a faster state response with better invariance properties against disturbances. The comparative simulation analysis of the proposed scheme with traditional SMC and PID control is also presented in this study. The numerical results illustrate the efficacy of the proposed fuzzy SMC technique over the other two in terms of convergence time, maximum overshoot, energy consumption, and chattering suppression. However, one of the shortcomings of this scheme is that only asymptotic convergence of system trajectories is ensured theoretically. Therefore, future extension of this work could be focused on achieving the finite time results for state response as well. Furthermore, system complexity could also be enhanced by considering rotor flexibility and gyroscopic effect.

Data availability statement

The raw data supporting the conclusion of this article will be made available by the authors, without undue reservation.

Author contributions

SS contributed to the conception, methodology, and design of the study. SS carried out the formal analysis. SS organized the database and software coding. SS and SA performed the mathematical analysis and theoretical investigation. SS realized the simulation results. SS wrote the first draft of the manuscript. SA, JB, AA, and MN wrote sections of the manuscript. SS and SA revised the manuscript and addressed the reviewer's comments. MN supervised this work. MN provided the laboratory resources. JB and AA arranged the funding. All authors contributed to manuscript revision and read and approved the submitted version.

Funding

The Deanship of Scientific Research at King Khalid University funded this work through Research Groups Program under grant no. RGP 2/91/43.

Acknowledgments

The authors extend their appreciation to the Deanship of Scientific Research at King Khalid University, Saudi Arabia, for funding this work through the Research Group Program under grant no. RGP 2/91/43.

Conflict of interest

The authors declare that the research was conducted in the absence of any commercial or financial relationships that could be construed as a potential conflict of interest.

Publisher's note

References

Abooee, A., and Arefi, M. M. (2019). Robust finite-time stabilizers for five-degree-of-freedom active magnetic bearing system. *J. Frankl. Inst.* 356, 80–102. doi:10.1016/j.jfranklin.2018.08.026

Aenis, M., Knopf, E., and Nordmann, R. (2002). Active magnetic bearings for the identification and fault diagnosis in turbomachinery. *Mechatronics* 12, 1011–1021. doi:10.1016/s0957-4158(02)00009-0

Alassar, A. Z., Abuhadrous, I. M., and Elaydi, H. A. (2010). "Modeling and control of 5 dof robot arm using supervisory control," in 2010 The 2nd International Conference on Computer and Automation Engineering (ICCAE) (IEEE), 351–355.

Amer, A. F., Sallam, E. A., and Elawady, W. M. (2011). Adaptive fuzzy sliding mode control using supervisory fuzzy control for 3 dof planar robot manipulators. *Appl. Soft Comput.* 11, 4943–4953. doi:10.1016/j.asoc.2011.06.005

Amrr, S. M., and Alturki, A. (2021). Robust control design for an active magnetic bearing system using advanced adaptive smc technique. *IEEE Access* 9, 155662–155672. doi:10.1109/access.2021.3129140

Amrr, S. M., Srivastava, J. P., and Nabi, M. (2020). Robust attitude stabilization of spacecraft under constrained network with hysteresis quantizer. *IEEE J. Miniat. Air Space Syst.* 2, 129–139. doi:10.1109/jmass.2020.3039977

Amrr, S. M., Ahmad, J., Waheed, S. A., Sarwar, A., Saidi, A. S., and Nabi, M. (2022a). Finite-time adaptive sliding mode control of a power converter under multiple uncertainties. *Front. Energy Res.* 10, 580. doi:10.3389/fenrg.2022.901606

Amrr, S. M., Alturki, A., and Zafar, K. (2022b). Advanced robust control design for the support of fast rotating shaft using active magnetic bearings. *Transp. Eng.* 10, 100139. doi:10.1016/j.treng.2022.100139

Amrr, S. M., Sarkar, R., Banerjee, A., Saidi, A. S., and Nabi, M. u. (2022c). Fault-tolerant finite-time adaptive higher order sliding mode control with optimized parameters for attitude stabilization of spacecraft. *Int. J. Robust Nonlinear Control* 32, 2845–2863. doi:10.1002/rnc.5934

Ang, K. H., Chong, G., and Li, Y. (2005). Pid control system analysis, design, and technology. *IEEE Trans. Control Syst. Technol.* 13, 559–576. doi:10.1109/tcst.2005.847331

Bai, Y., and Roth, Z. S. (2019). "Fuzzy logic control systems," in *Classical and modern controls with microcontrollers* (Springer), 437–511.

Bhat, S. P., and Bernstein, D. S. (2000). Finite-time stability of continuous autonomous systems. *SIAM J. Control Optim.* 38, 751–766. doi:10.1137/s0363012997321358

Bleuler, H., Cole, M., Keogh, P., Larsonneur, R., Maslen, E., Okada, Y., et al. (2009). *Magnetic bearings: Theory, design, and application to rotating machinery*. Verlag Berlin Heidelberg: Springer Science & Business Media.

Bonfitto, A., Castellanos Molina, L., Tonoli, A., and Amati, N. (2018). Offset-free model predictive control for active magnetic bearing systems. *Actuators* (Multidisciplinary Digital Publishing Institute), 7, 46.

Chang, L.-Y., and Chen, H.-C. (2009). Tuning of fractional pid controllers using adaptive genetic algorithm for active magnetic bearing system. *WSEAS Trans. Syst.* 8, 158–167.

Chen, K.-Y., Tung, P.-C., Tsai, M.-T., and Fan, Y.-H. (2009). A self-tuning fuzzy pid-type controller design for unbalance compensation in an active magnetic bearing. *Expert Syst. Appl.* 36, 8560–8570. doi:10.1016/j.eswa.2008.10.055

Cole, M. O., Chamroon, C., and Keogh, P. S. (2017). H-infinity controller design for active magnetic bearings considering nonlinear vibrational rotordynamics. *Mech. Eng. J.* 4, 16–00716. doi:10.1299/mej.16-00716

Davila, J., Fridman, L., and Levant, A. (2005). Second-order sliding-mode observer for mechanical systems. *IEEE Trans. Autom. Contr.* 50, 1785–1789. doi:10.1109/tac.2005.858636

De Miras, J., Join, C., Fliess, M., Riachy, S., and Bonnet, S. (2013). "Active magnetic bearing: A new step for model-free control," in 52nd IEEE Conference on Decision and Control (IEEE), 7449–7454.

Defoort, M., Floquet, T., Kokosy, A., and Perruquetti, W. (2009). A novel higher order sliding mode control scheme. *Syst. Control Lett.* 58, 102–108. doi:10.1016/j.sysconle.2008.09.004

Edwards, C., and Spurgeon, S. (1998). *Sliding mode control: theory and applications*. London: CRC Press.

Eker, I. (2006). Sliding mode control with pid sliding surface and experimental application to an electromechanical plant. *ISA Trans.* 45, 109–118. doi:10.1016/s0019-0578(07)60070-6

Esfahani, A. F., Jastrzebski, R. P., Kauranne, T., Haario, H., and Pyrhönen, O. (2013). "Novel methods of chaos detection of active magnetic bearing (amb) system by signal analysis," in 2013 15th European Conference on Power Electronics and Applications (EPE) (IEEE), 1–9.

Huang, J., Wang, L., and Huang, Y. (2007). Continuous time model predictive control for a magnetic bearing system. *PIERS online* 3, 202–208. doi:10.2529/piers060906214406

Kang, M. S., Lyou, J., and Lee, J. K. (2010). Sliding mode control for an active magnetic bearing system subject to base motion. *Mechatronics* 20, 171–178. doi:10.1016/j.mechatronics.2009.09.010

Kang, H., Oh, S.-Y., and Song, O. (2011). H∞ control of a rotor-magnetic bearing system based on linear matrix inequalities. *J. Vib. Control* 17, 291–300. doi:10.1177/1077546310362449

Knospe, C. R. (2007). Active magnetic bearings for machining applications. *IFAC Proc. Vol.* 15, 307–312. doi:10.1016/s1474-6670(17)31072-8

Koshizuka, N., Ishikawa, F., Nasu, H., Murakami, M., Matsunaga, K., Saito, S., et al. (2003). Progress of superconducting bearing technologies for flywheel energy storage systems. *Phys. C. Supercond.* 386, 444–450. doi:10.1016/s0921-4534(02)02206-2

Levant, A. (2003). Higher-order sliding modes, differentiation and output-feedback control. *Int. J. Control* 76, 924–941. doi:10.1080/0020717031000099029

Levant, A. (2007). Principles of 2-sliding mode design. *Automatica* 43, 576–586. doi:10.1016/j.automatica.2006.10.008

Li, H.-X., Gatland, H., and Green, A. (1997). Fuzzy variable structure control. *IEEE Trans. Syst. Man. Cybern. B* 27, 306–312. doi:10.1109/3477.558824

Lin, F., Chen, S., and Huang, M. (2010). Tracking control of thrust active magnetic bearing system via hermite polynomial-based recurrent neural network. *IET Electr. Power Appl.* 4, 701–714. doi:10.1049/iet-epa.2010.0068

Lin, F.-J., Chen, S.-Y., and Huang, M.-S. (2011). Intelligent double integral sliding-mode control for five-degree-of-freedom active magnetic bearing system. *IET control Theory & Appl.* 5, 1287–1303. doi:10.1049/iet-cta.2010.0237

Lin, B., Su, X., and Li, X. (2019). Fuzzy sliding mode control for active suspension system with proportional differential sliding mode observer. *Asian J. Control* 21, 264–276. doi:10.1002/asjc.1882

Liu, Y., Ming, S., Zhao, S., Han, J., and Ma, Y. (2019). Research on automatic balance control of active magnetic bearing-rigid rotor system. *Shock Vib.* 2019, 1–13. doi:10.1155/2019/3094215

Lo, J.-C., and Kuo, Y.-H. (1998). Decoupled fuzzy sliding-mode control. *IEEE Trans. Fuzzy Syst.* 6, 426–435. doi:10.1109/91.705510

Mushi, S. E., Lin, Z., and Allaire, P. E. (2011). Design, construction, and modeling of a flexible rotor active magnetic bearing test rig. *Ieee. ASME. Trans. Mechatron.* 17, 1170–1182. doi:10.1109/tmech.2011.2160456

Noshadi, A., Shi, J., Poolton, S., Lee, W., and Kalam, A. (2014). "Comprehensive experimental study on the stabilization of active magnetic bearing system," in 2014 Australasian Universities Power Engineering Conference (AUPEC) (IEEE), 1–7.

Palm, R. (1994). Robust control by fuzzy sliding mode. *Automatica* 30, 1429–1437. doi:10.1016/0005-1098(94)90008-6

Peng, C., and Zhou, Q. (2019). Direct vibration force suppression for magnetically suspended motor based on synchronous rotating frame transformation. *IEEE Access* 7, 37639–37649. doi:10.1109/access.2019.2904745

Polajžer, B., Ritonja, J., Štumberger, G., Dolinar, D., and Lecointe, J.-P. (2006). Decentralized pi/pd position control for active magnetic bearings. *Electr. Eng.* 89, 53–59. doi:10.1007/s00202-005-0315-1

Qin, H.-l., Li, Z.-x., and Yuan, S. (2011). Application research of fuzzy sliding model control for active magnetic bearings. *Comput. Simul.* 48.

Ricci, M. R., Antaki, J. F., Verkaik, J. E., Paden, D. B., Snyder, S. T., Paden, B. E., et al. (2016). Magnetically-levitated blood pump with optimization method enabling miniaturization. US Patent 9,314,557. [Dataset]

Roopaei, M., and Jahromi, M. Z. (2009). Chattering-free fuzzy sliding mode control in mimo uncertain systems. *Nonlinear Analysis Theory, Methods & Appl.* 71, 4430–4437. doi:10.1016/j.na.2009.02.132

Saha, S., and Nabi, M. (2016). "A review on active magnetic bearing and exploitation of parametric model order reduction," in IEEE proc. 11th International Conference on Industrial and Information Systems (ICIIS), Roorkee, India, 420–425.

Saha, S., Amrr, S. M., Nabi, M., and Iqbal, A. (2019). Reduced order modeling and sliding mode control of active magnetic bearing. *IEEE Access* 7, 113324–113334. doi:10.1109/access.2019.2935541

Saha, S., Amrr, S. M., and Nabi, M. (2020). Adaptive second order sliding mode control for the regulation of active magnetic bearing. *IFAC-PapersOnLine* 53, 1–6. doi:10.1016/j.ifacol.2020.06.001

Saha, S., Amrr, S. M., Saidi, A. S., Banerjee, A., and Nabi, M. (2021). Finite-time adaptive higher-order smc for the nonlinear five dof active magnetic bearing system. *Electronics* 10, 1333. doi:10.3390/electronics10111333

Scharfe, M., Roschke, T., Bindl, E., and Blonski, D. (2001). "Design and development of a compact magnetic bearing momentum wheel for micro and small satellites," in 15th Annual/USU Conference on Small Satellites.

Sharma, A., Amrr, S. M., Nabi, M., and Banerjee, S. (2021). "Extended state observer based integral sliding mode control of maglev systems with enhanced chattering alleviation," in 2021 Seventh Indian Control Conference (ICC) (IEEE), 242–247.

Sharma, A., Alturki, A., and Amrr, S. M. (2022). Extended state observer based integral sliding mode control for maglev system with fixed time convergence. *IEEE Access* 10, 93074–93083. doi:10.1109/access.2022.3204059

Shtessel, Y., Edwards, C., Fridman, L., and Levant, A. (2014). *Sliding mode control and observation*. New York: Springer.

Sivrioglu, S. (2007). Adaptive backstepping for switching control active magnetic bearing system with vibrating base. *IET Control Theory & Appl.* 1, 1054–1059. doi:10.1049/iet-cta:20050473

Stepanenko, Y., Cao, Y., and Su, C.-Y. (1998). Variable structure control of robotic manipulator with pid sliding surfaces. *Int. J. Robust Nonlinear Control* 8, 79–90. doi:10.1002/(sici)1099-1239(199801)8:1<79:aid-rnc313>3.0.co;2-v

Su, K.-H., and Li, C.-Y. (2016). "Supervisory fuzzy model control for magnetic levitation system," in 2016 IEEE 13th International Conference on Networking, Sensing, and Control (ICNSC) (IEEE), 1–6.

Tang, J., Xiang, B., and Zhang, Y. (2014). Dynamic characteristics of the rotor in a magnetically suspended control moment gyroscope with active magnetic bearing and passive magnetic bearing. *ISA Trans.* 53, 1357–1365. doi:10.1016/j.isatra.2014.03.009

Tong, S., and Li, H.-X. (2003). Fuzzy adaptive sliding-mode control for mimo nonlinear systems. *IEEE Trans. Fuzzy Syst.* 11, 354–360. doi:10.1109/tfuzz.2003.812694

Utkin, V., Poznyak, A., Orlov, Y., and Polyakov, A. (2020). Conventional and high order sliding mode control. *J. Frankl. Inst.* 357, 10244–10261. doi:10.1016/j.jfranklin.2020.06.018

Wang, L.-X., and Mendel, J. M. (1992). Generating fuzzy rules by learning from examples. *IEEE Trans. Syst. Man. Cybern.* 22, 1414–1427. doi:10.1109/21.199466

Xu, Y., and Nonami, K. (2003). A fuzzy modeling of active magnetic bearing system and sliding mode control with robust hyperplane using μ-synthesis theory. *JSME Int. J. Ser. C* 46, 409–415. doi:10.1299/jsmec.46.409

Yau, H.-T., and Chen, C.-L. (2006). Chattering-free fuzzy sliding-mode control strategy for uncertain chaotic systems. *Chaos, Solit. Fractals* 30, 709–718. doi:10.1016/j.chaos.2006.03.077

Zadeh, L. A. (1965). Fuzzy sets. *Inf. control* 8, 338–353. doi:10.1016/s0019-9958(65)90241-x

10.3389/fcteg.2022.1008134

Nomenclature

$\underline{n}$ upper bound of lumped uncertainty
$\boldsymbol{a}$ length between COG and left RAMB
$\boldsymbol{A}$ stiffness matrix
$\boldsymbol{A}_{nom}$ and $\boldsymbol{B}_{nom}$ nominal values of $\boldsymbol{A}$ and $\boldsymbol{B}$
$\boldsymbol{B}$ control gain matrix
$\boldsymbol{b}$ length between COG and right RAMB
$\boldsymbol{c}$ distance between COG and end of the rotor
$\boldsymbol{d}$ diameter of the rotor
$\boldsymbol{e}$ error
$\boldsymbol{G}_q$ auxiliary control gain
$\boldsymbol{i}_{x1}$ control current for state x_1
$\boldsymbol{J}$ transverse moment of inertia about the X and Y axis
$\boldsymbol{J}_z$ polar moment of inertia about the Z axis
$\boldsymbol{K}_d$ derivative gain
$\boldsymbol{k}_{fi}$ current stiffness of RAMB
$\boldsymbol{k}_{fp}$ position stiffness of RAMB
$\boldsymbol{K}_i$ integral gain
$\boldsymbol{K}_p$ proportional gain
$\boldsymbol{k}_{ti}$ current stiffness of TAMB
$\boldsymbol{k}_{tp}$ position stiffness of TAMB
$\boldsymbol{l}$ distance between left RAMB and right RAMB
$\boldsymbol{L}$ length of the rotor
$\boldsymbol{M}$ mass matrix
$\boldsymbol{m}$ mass of the rotor
$\boldsymbol{n}$ lumped uncertainty
$\boldsymbol{q}$ term due to decoupling
$\boldsymbol{s}$ sliding surface
$\boldsymbol{u}$ control inputs
$\boldsymbol{u}_q$ output of fuzzy SMC block
$\boldsymbol{x}$ states